THE IMPACT OF AGRICULTURAL EROSION PROCESSES UPON $\delta^{15}N$, $\delta^{13}C$, AND C/N SIGNATURES OF ERODED-SOIL

J.F. Fox, Dept. of Civil Engineering, University of Kentucky, Lexington, Kentucky; A.N. Papanicolaou, IIHR-Hydroscience & Engineering, Dept. of Civil Engineering, The University of Iowa, Iowa City, Iowa

Abstract: The objective here is to show the ability of $\delta^{15}N$, $\delta^{13}C$, and C/N to capture the response of morphologic erosion processes. Analyses of $\delta^{15}N$, $\delta^{13}C$, and C/N of suspended eroded-soils, upland soils, and floodplain soils illustrate that an early event on March 7th 2003 was indicative of non-equilibrium sediment transport conditions. Later events on March 14th and 22nd produce eroded-soil in quasi-equilibrium conditions that may be predicted using rill erosion and headcut erosion models. It is expected that the sensitivity of $\delta^{15}N$, $\delta^{13}C$, and C/N will serve the purpose of sediment transport model calibration for further studying morphologic erosion processes.

INTRODUCTION

This work studies the ability of stable nitrogen and carbon isotopes, $\delta^{15}N$, $\delta^{13}C$, and the carbon to nitrogen atomic ratio, C/N, to capture the response of morphologic surface erosion processes. Connecting the response of $\delta^{15}N$, $\delta^{13}C$, and C/N with the soil erosion mechanisms will allow calibration of sediment transport models for landscape degradation and organic matter supply to streams.

In the Northwestern Wheat and Range Region (NWRR) of the Upper Palouse Basin, winter rill erosion is the major form of soil production and has been the topic of much research for the past three decades (Wischmeier & Smith 1978, McCool et al. 1993, McCool et al. 2000). Recently, research findings show that active floodplains may also produce significant production of soil in NWRR (Nagle & Ritchie 2004). The connectivity between upland and floodplain erosion processes is realized (Lauer & Parker 2005). Water and eroded-soil produced in upland rilling is either routed within swales and ditches through flow convergence or is deposited upon floodplain regions at the toe slope through flow divergence. In the latter, rills transition to sheet flow with a change in slope from the upland to the floodplain landforms. In active floodplains, headcuts are initiated at the edge of the floodplain near the streambank when raindrop energy produces a perturbation that initiates migration. Thereafter the floodplain sheet flow supplies headcuts with the energy needed to scour and migrate upslope.

$\delta^{15}N$, $\delta^{13}C$, and C/N are soil organic matter (SOM) signatures, which retain characteristics of vegetation and SOM processes (e.g. decomposition). $\delta^{15}N$, $\delta^{13}C$, and C/N studies have exhibited the sensitivity of the biogeochemicals to uniquely characterize upland and floodplain regions in the Upper Palouse (Fox & Papanicolaou, In Review). Therefore the use of $\delta^{15}N$, $\delta^{13}C$, and C/N to differentiate rill erosion from uplands and headcut erosion from floodplains is realized.

The objective here is to show the ability of $\delta^{15}N$, $\delta^{13}C$, and C/N to capture the response of rill erosion and headcut migration. This goal is facilitated by analyses of $\delta^{15}N$, $\delta^{13}C$, and C/N from eroded-soils, upland slope soil, and floodplain soil. These results are compared with erosion estimates based on rill erosion and headcut models.

METHODS

Study site: The Upper Palouse Watershed, Northwestern Idaho, is the target location. The Palouse River originates in the Palouse Mountain Range within the St. Joe National Forest northeast of Moscow, Idaho, and then flows west into Eastern Washington. Rolling hills used for agriculture (primarily winter wheat and hay) dominate in the downstream portions of the watershed. The hills have 15.6 % to 27.9 % steepness at approximately 750 m above mean sea level. Research indicates that as much as 90% of the soil loss in the Palouse region is caused by rainfall, and snowmelt upon thawing surface soils during late winter-early spring events (Wischmeier & Smith 1978, McCool et al. 2000). For this study, a small primarily agriculture sub-watershed (area equals about 1 km^2) in the Upper Palouse is focused for sampling and modeling, near Harvard, Idaho. Herein is referred to as the "Harvard Creek" sub-watershed.

Field sampling: Sampling of upland and floodplain soils and eroded-soil during the events of March 2003 was performed in the Harvard Creek sub-watershed. Upland and floodplain soil sampling methods followed protocols of pedologic and environmental scientists (Pansu & Loyer 2001, USDA 1993). For each sample, soil pits were excavated and samples were removed from the 0-5 cm level, omitting the root mat. An *in situ* suspended eroded-soil trap was installed at the outlet of Harvard Creek sub-watershed. The traps function as integrated samplers; and soil settles within the traps over the duration of the sampling period (Phillips et al. 2000). The soil traps were placed at the sub-watershed outlets on March 7, 2003, and eroded-soil was removed from the traps on March 14th on March 19th and again on April 2, 2003 constituting three sampling intervals. Water-soil samples were centrifuged in a high volume rotor to concentrate the soils and then freeze-dried.

Lab analyses: Samples were wet sieved within a Na-hexametaphosphate solution to retain the cohesive soil fraction (d<53 μm) (Cambardella & Elliott 1992), and ground on an orbital ball-mill in preparation for isotopic analysis. Samples were analyzed for isotope and elemental analyses at the University of Idaho Natural Resources Stable Isotope Laboratory. Precision of this method is typically better than 0.2‰ for nitrogen and 0.1‰ for carbon (Stickrod & Marshall 2000). Carbon and nitrogen stable isotopes are expressed in "*delta*" (δ) notation to indicate depletion (-) or enrichment (+) of the heavy (higher-mass) stable isotopes (^{13}C, ^{15}N) compared to the lighter-mass stable isotopes (^{12}C, ^{14}N). The *delta* notation (δ) refers to differences between the isotopic ratio of the sample and accepted standard materials expressed as:

$$\delta X\ (in\ ‰) = \left(\frac{R_{sample}}{R_{std}} - 1 \right) \bullet 10^3 \qquad (1)$$

where X is ^{13}C or ^{15}N, R_{sample} is the isotope ratio ($^{13}C/^{12}C$, or $^{15}N/^{14}N$) of the sample and R_{std} is the isotope ratio of the standard (Vienna Pee Dee Belemnite, VPDB, and atmospheric nitrogen, respectively). C/N is expressed in the form of an atomic ratio and is dimensionless.

RESULTS

Isotope results: Figure 1 plots the daily precipitation for the Upper Palouse from March 1 to April 2, 2003 as reported at the 15-minute rain gauge at Moscow, ID. Three peak storms are noticed in the plot on March 7th, March 15th, and March 22nd as well as a number of small daily precipitation accumulations. The nature of all storms was low intensity, long duration precipitation, typical of winters in the Upper Palouse. For example, the maximum peak shown in Figure 1 was a 17 hr storm on March 7th where 38.1 mm of rain fell on the Upper Palouse with a maximum intensity of 10.15 mm/hr occurring for a 15-minute period during hour 15 of the storm. During March 2003, soil temperatures did not fall below freezing.

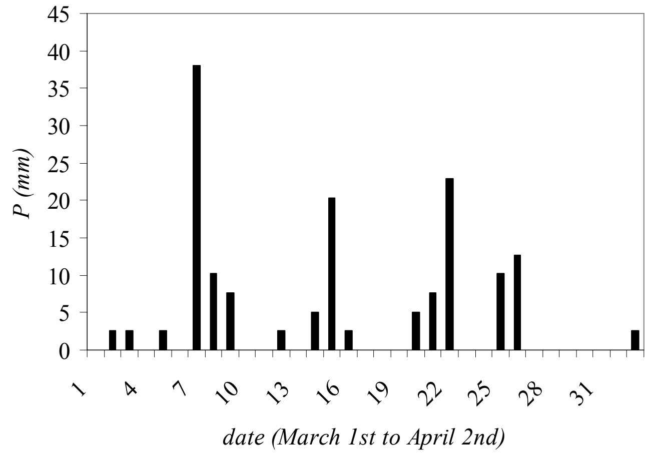

Figure 1 Daily precipitation for March 2003.

Table 1 shows eroded-soil data captured at the sub-watershed outlet for three intervals. Notice that each interval captures one of the three highest daily precipitation values as well as a number of the smaller daily precipitation accumulations. During the first interval (March 7th to March 14th) 37.51 g of eroded-soil was captured by the soil trap, which continuously captures sediment from a point in-stream, and when normalized by precipitation shows 0.59 g/mm. This first interval of sampling was a high erosion period followed by two lower rather consistent erosion periods. The early high erosion is attributed to non-equilibrium conditions when loose material on the soil surface and in swales, gullies, and ditches is eroded, rills are scouring and forming, and headcutting is occurring in active floodplains. A similar process has been observed by Romkens et al. (1997). The latter erosion periods (March 14 to 19 and March 19 to April 2) are attributed to further rill and headcut erosion under quasi-equilibrium conditions. For all samples approximately 90% of the eroded-soil was less than 53μm (see Table 1) in size constituting silt and clay size-fraction. The 90% fines data agrees with soil in the region where 85 to 90% of the soil is dominated by the silt and clay fractions. Further observations of the soil samples reveal that the average size of the eroded material for the March 14 to 19 and March 19-Apr 2 events increases comparatively to the March 7 to 14. This is attributed to the fact that during the March 7 to 14 event the finer, looser soil aggregates found atop of the soil surface are entrained by the flow. Based on weather records from Moscow, temperatures fluctuated between freezing and thawing conditions for soil in February 2003 and early March with only small amounts of daily precipitation and little to no erosion. The freezing-thawing tended to break soil aggregates on the surface exposing the loose fine material. The storm on March 7th eroded this material, which is well represented with the $\delta^{15}N$, $\delta^{13}C$, and C/N data. During the March 14 to 19 and March 19 to -April 2 events the soil seals and the transport of the material is at equilibrium and the transported material is overall coarser in size.

Table 1 Eroded-soil data captured at the Harvard Creek sub-watershed outlet.

Sampling interval	Mass g	Mass/P g/mm	*d*<53μm %
March 7 to 14	37.51	0.59	93
March 14 to 19	5.49	0.24	89
March 19-Apr 2	11.96	0.20	90

Table 2 presents $\delta^{15}N$, $\delta^{13}C$, and C/N data for eroded-soils captured at Harvard Creek sub-watershed outlet for the three sampling intervals. Notice the higher $\delta^{15}N$ and $\delta^{13}C$ values and lower C/N value for the first interval (March 7th to 14th) as compared to the second and third intervals. The degraded signature of $\delta^{15}N$, $\delta^{13}C$, and C/N is attributed to particle size of eroded material pointed out earlier. Past studies have shown that organic matter decreases in size as degradation persists, and finer organic matter has higher $\delta^{15}N$ and $\delta^{13}C$ values and lower C/N value as compared to coarser organic matter (Turchenek & Oades 1979, Balesdent & Mariotti 1996, Yoneyama 1996, Stevenson 1997). The finer sized, degraded soils that eroded during the first interval are explained based on the non-equilibrium conditions discussed above. In short, the results in Table 2 show that there is a correspondence between soil size and biogeochemical signatures during erosion. This supports the findings of the preliminary soil analysis and illustrates the uniqueness of the $\delta^{15}N$, $\delta^{13}C$, and C/N to differentiate soils of different size.

Table 2 $\delta^{15}N$, $\delta^{13}C$, and C/N for eroded-soils captured at the Harvard Creek sub-watershed outlet.

Sampling interval	$\delta^{15}N$ ‰	$\delta^{13}C$ ‰	C/N --
March 7 to 14	4.23	-25.99	10.48
March 14 to 19	2.71	-26.64	14.35
March 19-Apr 2	2.59	-26.92	13.05

The $\delta^{15}N$, $\delta^{13}C$, and C/N data in Table 2 may be compared with mean estimates for $\delta^{15}N$, $\delta^{13}C$, and C/N of soils in Harvard Creek sub-watershed. Table 3 shows means estimates at two sampling depths for upland slope and floodplain samples. In general the soil data do not compare well with the March 7 to 14 eroded-soil data indicative of the non-equilibrium conditions. The soil data compare better with eroded-soil data from the later sampling intervals. During this time, erosion occurs from rill down-cutting and headcuts under quasi-equilibrium conditions.

Table 3 δ^{15}N, δ^{13}C, and C/N mean estimates for upland and floodplain soils in Harvard Creek sub-watershed.

Source	δ^{15}N ‰	δ^{13}C ‰	C/N --
Upland slopes	2.87	-26.23	12.64
Floodplains	2.00	-27.02	11.98

Modeling erosion processes: The analyses of δ^{15}N, δ^{13}C, and C/N from eroded-soils, upland slope soil, and floodplain soil is complemented with modeling. This modeling is restricted to the equilibrium events, March 14 to 19 and March 19 to -April 2 events, since existing modeling capabilities do not permit simulation of non-equilibrium conditions. Rill erosion and headcut modeling are performed to estimate the relative contribution of the uplands and floodplains to the eroded-soil.

The Water Erosion Prediction Project (WEPP) erosion model is used to predict the contribution of soil from rill erosion for the storms in March 14 to 19 and March 19 to -April 2; and thereafter headcut migration is predicted using equilibrium equations from Alonso & Bennett (2002). WEPP solves the sediment continuity equation for rill erosion and provides results of rill width and depth within a hill slope profile. A comprehensive review of the model formulation is available in Foster et al. (2005). The driving sediment equations for rill erosion in the model includes the steady-state sediment continuity equation for a hill slope given as:

$$\frac{dG}{dx} = D_f \tag{2}$$

where G is sediment load and D_f is rill erosion rate. The interill contribution is not considered here because interills have a minimal erosion comparatively to rills during the winter period that extends up to April 15 (McCool et al. 1993). D_f is either detachment in rills when the applied hydraulic shear stress exceeds the critical shear stress of the soil and when the sediment load is less than the sediment carrying capacity. Rill detachment is:

$$D_f = K_r\left(\tau_f - \tau_c\right)\left(1 - \frac{G}{T_c}\right) \tag{3}$$

where K_r is a rill erodibility parameter, τ_f is flow shear stress, τ_c is the critical shear stress, and T_c is sediment transport capacity. Net deposition in the rill is computed when sediment load, G, is greater than sediment transport capacity, T_c. The equation for deposition follows:

$$D_f = \frac{\beta V_f}{q}\left(T_c - G\right) \tag{4}$$

where V_f is the effective fall velocity for the sediment, q is unit discharge in the rills, and β is a raindrop-induced turbulent coefficient. WEPP allows for specification of climate, agriculture management, and soil parameters that correspond to the conditions of the Upper Palouse. From the WEPP analysis, the maximum depth of rill erosion, D_{mf}, may be calculated after budgeting deposition and detachment as well as the sediment yield, S_y, from the rills.

Because upland and floodplain erosion processes are physically connected, the results from the WEPP model are used to drive headcut migration. Rills provide the fluid power to maintain headcut migration after raindrop splash has initiated movement near the edge of the floodplains. Thus runoff results produced from the WEPP simulations were used with headcut relationships from Alonso & Bennett (2002) to assess the maximum depth and sediment yield from migrating headcuts. The equilibrium depth of scour, S_D, is given by:

$$S_D = \sigma V_e q_w^{4/5} sin\theta_e + h \quad (5)$$

where

$$\sigma = \frac{c_d^2 \delta_f \rho_w \nu^{1/5}}{2(\tau_c / \beta)}, \quad (6)$$

and q_w is unit discharge at the base of the slope and is calculated using a peak discharge equation, c_d is the turbulent diffusion coefficient of a submerged jet, ρ_w and ν are the density and kinematic viscosity of water, τ_c is the critical shear stress of the soil, δ_f and β are calibrating coefficients, V_e is the average jet velocity, θ_e is the jet entry angle, and h is the vertical distance from the brink to tailwater surface. The equilibrium migration rate, M, of a headcut is given by:

$$M = V_e \sqrt{\frac{\mu q_w}{S_D - h}} \quad (7)$$

where

$$\mu = \frac{1}{2} \rho_w k_d \sin^2 \frac{\theta_e}{2} \quad (8)$$

and k_d is the soil erodibility coefficient.

A sensitivity analysis was performed for WEPP in order to identify the critical parameters controlling the maximum depth of rill erosion, D_{mf}. Input parameters including critical shear stress of rill soils, τ_{cr}, rill width, w_r, initial soil saturation, s_i, and initial conditions for agriculture management were varied to assess outputs including the maximum depth of rill erosion, D_{mf}, and sediment yield, S_y. The model is most sensitive to initial management conditions and τ_{cr} with less sensitivity to w_r. Initial conditions of live winter wheat in a continuous wheat rotation was used for management based on consultation with local farmers and a value of 0.1 Pa was

specified for τ_{cr} (Papanicolaou, unpublished). Based on the prevailing hydrologic conditions a value of 100% for s_i was considered.
Uncertainty exists for the percent occurrence of headcut initiation and migration in the floodplains (or equivalently for the percentage of the floodplain area covered by headcuts). Headcut occurrence needs further research. For the conditions here, a range of 5 to 25% headcut occurrence was specified.

In this analysis, the agriculture hill slopes was simulated to assess maximum rill erosion depth, D_{mf}, and sediment yield, S_y, for the March 14 to 19 and March 19 to -April 2 events. The hill slope was modeled with slope and slope length values of 28.4% and 51 m, respectively, corresponding to mean values for the region (McCool et al. 1993). Climate data were used for the model based on analysis of 15-minute rain gage data from Moscow, ID.

Maximum erosion depths were output for the events. D_{mf} and S_D were 3mm and 3mm for March 14 to 19; and D_{mf} and S_D were 10mm and 7mm for March 19 to -April 2 indicating the maximum scour depths for the rill and headcut processes.

The mass percent of sediment yield from the headcuts and sediment yield from the rills was calculated for the modeling results. Sediment yield from the headcuts accounted for only 2 to 10% of the sediment load depending on the storm modeled and the percent cover specified for the migrating headcuts. The small contribution from the headcuts in the floodplains exhibits the dominance of the rill erosion in the region as reported by McCool et al. (1993).

Mass balance for rills and headcuts: The upland and floodplain soils can now be weighted in order that results may be compared with the $\delta^{15}N$, $\delta^{13}C$, and C/N signature of eroded-soil. A mass balance is performed for $\delta^{15}N$, $\delta^{13}C$, and C/N by specifying the contribution from the rills and headcuts. The equation follows:

$$y^j = \sum_{i=1} \alpha_i x_i^j \quad \text{where} \quad \sum \alpha_i = 1 . \tag{9}$$

In Equation (1), y^j specifies the j=3 tracers, $\delta^{15}N$, $\delta^{13}C$, and C/N, x_i^j is the mean value for the upland and floodplain tracers where i=2 to indicate the two sources (i.e. headcuts and rills) and α_i is the mass fraction of eroded-soil for each source; here 0.94 and 0.06 are specified for the rills and headcuts, respectively. Results indicate values of 2.82‰, -26.60‰, and 12.60 for $\delta^{15}N$, $\delta^{13}C$, and C/N of the eroded-soil. Comparison with Table 2 indicates that better agreement between simulated and observed data is found by including the contribution from the two sources.

CONCLUSIONS

The objective here was to show the ability of $\delta^{15}N$, $\delta^{13}C$, and C/N to capture the response of rill erosion and headcut migration. The early event on March 7th produced eroded-soil that is not indicative of $\delta^{15}N$, $\delta^{13}C$, and C/N of upland or floodplain soils due to the persistence of non-equilibrium conditions. For the latter events on March 14th and March 22nd results indicate that a mass balance, which accounts for multiple sources, here uplands and floodplains, will produce results that more accurately represent $\delta^{15}N$, $\delta^{13}C$, and C/N of eroded-soil. Uncertainty analysis in future work will complement the results herein.

This work exhibits the utility of $\delta^{15}N$, $\delta^{13}C$, and C/N of eroded-soil to be used in sediment transport model calibration and for studying morphologic erosion processes. It is expected that the sensitivity of the bio-geochemicals will serve to better elucidate the processes controlling sediment transport phenomena.

REFERENCES

Alonso, C. V. & Bennett, S. J. 2002. "Predicting headcut migration in concentrated flows typical of upland areas," Water Resources Research, 38(12): 39-1-15.

Balesdent, J., & Mariotti, A. 1996. "Measurement of SOM Turnover Using 13C Natural Abundance. In: Mass Spectrometry of Soils," (eds Boutton, T. W. & Yamasaki, S. I.), Marcel Dekker, New York, pp 83-111.

Cambardella, C. A., & Elliott, E. T. 1993. "Particulate soil organic-matter changes across a grassland cultivation sequence," Soil Sci Soc Am J., 56: 777-783.

Foster, G.R., Flanagan, D.C., Nearing, M.A., Lane, L.J., Risse, L.M., & Finkner, S.C. 1995. "Chapter 11. Hillslope erosion component," In WEPP Technical Document, USDA-ARS, July 2005.

Fox, J. F. & Papanicolaou, A. N. "Factors controlling statistical variability of $\delta^{15}N$, $\delta^{13}C$, and C/N among agriculture and forest soils within the Upper Palouse Watershed, Northwestern Idaho," In review at Hydrologic Processes.

Lauer, J.W. & Parker, G. 2005. "Net transfer of sediment from floodplains to channels on three southern US rivers," Presented at World Waters and Environmental Resources Congress, May 15-19, Anchorage, Alaska.

McCool, D. K., George, G.O., Freckleton, M., Douglas, C.L., & Papendick, R.I. 1993. "Topographic effect on erosion from cropland in the Northwestern Wheat Region," Transactions of the ASAE, 36(4): 1067-1071.

McCool, D.K., Pannkuk, C.D., Saxton, K.E., & Kalita, P.K. 2000. "Winter Runoff and Erosion on Northwestern USA Cropland," International Journal of Sediment Research. 15(2), 149-161.

Nagle & Ritchie, 2004. "Wheat field erosion rates and channel bottom sediment sources in an intensively cropped Northeastern Oregon drainage basin," Land Degradation & Development, 15: 15-26.

Pansu, M., Gautheyrou, & J., Loyer, J-Y. 2001. Soil Analysis. A. A. Balkema Publishers, Lisse.

Phillips, J.M., Russell, M.A., & Walling, D.E. 2000. "Time-integrated sampling of fluvial suspended sediment: a simple methodolgy for small catchments," Hydrological Processes, 14, 2589-2602.

Romkens, M.J.M., Prasad, S.N., & Gerits, J.J.P. 1997. "Soil erosion modes of sealing soils: a phenomenological study," Soil Technology, 11:31-41.

Stevenson, B. 1997. "Stable carbon and oxygen isotopes in soils and paleosols of the Palouse loess, Eastern Washington State: Modern relationships and applications for paleoclimatic reconstruction," Ph. D Thesis, Colorado State University.

Stickrod II, R.D. & Marshall, J.D. 2000. "On-line nitrate-$\delta^{15}N$ extracted from groundwater determined by continuous-flow elemental analyzer/isotope ratio mass spectrometry," Rapid

Communications in Mass Spectrometry. 14, 1266-1268.
Turchenek, L.W. & Oades, J.M. 1979. "Fractionation of organo-mineral complexes by sedimentation and density techniques," Geoderma. 21, 311-343.
United States Department of Agriculture (USDA). 1993. Soil Survey Manual.
Wischmeier & Smith. 1978. "Predicting rainfall erosion losses: A guide to conservation planning," USDA, Agriculture Handbook, No. 537. US Government Printing Office, Washington, DC.
Yoneyama, T. 1996. "Characterization of natural 15N abundance of soils," In: Mass Spectrometry of Soils. (eds Boutton, T. W. & Yamasaki, S. I.), Marcel Dekker, New York, pp 205-224.